"Lithio-Aversion" of Thiophene Sulfur Atoms in the X-ray Crystal Structures of $[Li-O-SiMe_2(2\text{-}C_4H_3S)]_6$ and $[Li-O-CH(i\text{-}Pr)(2\text{-}C_4H_3S)]_6$: Models for Electrostatic Metal−Thiophene Interactions

Bernd Goldfuss, Paul von Ragué Schleyer,* and Frank Hampel

Institut für Organische Chemie der Universität Erlangen-Nürnberg, Henkestrasse 42, D-91054 Erlangen, Germany

Received April 28, 1997[⊗]

Although lithium−sulfur interactions should result if the thienyl groups in $[Li-O-SiMe_2\text{-}(2\text{-}C_4H_3S)]_6$ ((**6**)$_6$) and in $[Li-O-CH(i\text{-Pr})(2\text{-}C_4H_3S)]_6$ ((**9**)$_6$) were rotated, no short distances between the lithiums of the $(LiO)_6$ cores and the thiophene S atoms (Li−S > 3 Å) are apparent in their X-ray crystal structures. Instead, the thienyl conformations in (**9**)$_6$ benefit from Li (C═C) π-interactions ($Li_1-C_2 = 2.631(7)$ Å, $Li_1-C_3 = 2.845(7)$ Å). DFT (B3LYP) computations show Li−S contacts to be only slightly favored over Li−C binding in $Li-O-SiH_2(2\text{-}C_4H_3S)$ (**7**) (1.4 kcal/mol) and in $Li-O-CH_2(2\text{-}C_4H_3S)$ (**8**) (1.7 kcal/mol). Semiempirical PM3 conformational analyses of thienyl groups on the $(LiO)_6$ cores of the model hexamers $[Li-O-SiH_2\text{-}(2\text{-}C_4H_3S)]_6$ (**7**)$_6$ and $[Li-O-CH_2(2\text{-}C_4H_3S)]_6$ ((**8**)$_6$) show preferences for pyramidal Li−S(thiophene) contacts, whereas planar Li−O arrangements are favored for the furanyl analogues. Due to the higher aromaticity of thiophene, the σ "in-plane" Li^+−S(thiophene) coordination energy ($Li^+-SC_4H_4$, 16.9 kcal/mol) is reduced relative to that of the Li^+-SMe_2 reference (29.5 kcal/mol) more than is the less aromatic furan ($Li^+-OC_4H_4$, 29.2 kcal/mol) relative to Li^+-OMe_2 (39.1 kcal/mol). Consistently, the Li^+ π-coordination affinity of thiophene (32.1 kcal/mol) is higher than that of furan (29.6 kcal/mol). The electrostatic potential (EP) of thiophene is only slightly negative in the ring plane at sulfur but considerably more negative in the "out-of-plane" π-region. This rationalizes the "lithio-aversion" of thienyl sulfur atoms in the X-ray crystal structures of (**6**)$_6$ and of (**9**)$_6$: electrostatic metal−thiophene interactions favor the thiophene π-system rather than the "in-plane" sulfur region.

Introduction

The electrostatic contributions[1] to metal−thiophene interactions are best revealed in alkali-metal[2] thiophene complexes. In contrast to the large number of thiophene−transition-metal X-ray crystal structures, the 2-lithiobenzothiophene−tmeda species **1-S**[3] is the only alkali-metal thiophene system that has been investigated structurally.

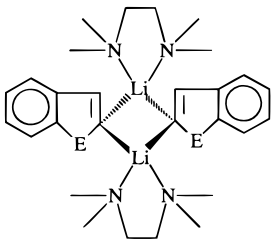

E = S **(1-S)**, O **(1-O)**

Interactions of thiophenes with transition-metal sulfide surfaces play a key role in the catalytic hydrodesulfurization of petroleum feedstocks.[4] In order to gain knowledge about bonding and activation of thiophene ligands and to model early stages of the hydrodesulfur ization process, a variety of transition-metal complexes have been synthesized and η^1 (S),[5] η^2 (C═C),[6] η^4 (c-{C_4S}),[7] and η^5 (c-{C_4S})[8] coordination modes were identified.

These interactions increase the susceptibility of the thiophene ligands to nucleophilic attack,[9] they result in

[⊗] Abstract published in *Advance ACS Abstracts,* October 1, 1997.

(1) Electrostatic contributions to metal−cyclopropane and metal−acetylene interactions are discussed in: (a) Goldfuss, B.; Schleyer, P. v. R.; Hampel, F. *J. Am. Chem. Soc.* **1996**, *118*, 12183. (b) Goldfuss, B.; Schleyer, P. v. R.; Hampel, F. *J. Am. Chem. Soc.* **1997**, *119*, 1072.

(2) For reviews see: (a) Sapse, A.-M., Schleyer, P. v. R., Eds. *Lithium Chemistry*; Wiley: New York, 1995. (b) Lambert, C.; Schleyer, P. v. R. *Angew. Chem.* **1994**, *106*, 1187; *Angew. Chem., Int. Ed. Engl.* **1994**, *33*, 1129. (c) Lambert, C.; Schleyer, P. v. R. *Methods of Organic Chemistry (Houben-Weyl)*; 4th ed.; Thieme: Stuttgart, Germany, 1993; Vol. E19d, p 1. (d) Weiss, E. *Angew. Chem.* **1993**, *105*, 1565; *Angew. Chem., Int. Ed. Engl.* **1993**, *32*, 1501. (e) Gregory, K; Schleyer, P. v. R.; Snaith, R. *Adv. Inorg. Chem.* **1991**, *37*, 47. (f) Schade, C.; Schleyer, P. v. R. *Adv. Organomet. Chem.* **1987**, *27*, 169. (g) Setzer, W. N.; Schleyer, P. v. R. *Adv. Organomet. Chem.* **1985**, *24*, 353.

(3) Harder, S.; Boersma, J.; Brandsma, L.; Kanters, J. A.; Bauer, W.; Pi, R.; Schleyer, P. v. R.; Schöllhorn, H.; Thewalt, U. *Organometallics* **1989**, *8*, 1688.

(4) (a) Harris, S. *Organometallics* **1994**, *13*, 2628. (b) Wiegand, B. C.; Friend, C. M. *Chem. Rev.* **1992**, *92*, 491. (c) Rauchfuss, T. B. *Prog. Inorg. Chem.* **1991**, *39*, 259. (d) Angelici, R. J. *Coord. Chem. Rev.* **1990**, *105*, 61. (e) Angelici, R. J. *Acc. Chem. Res.* **1988**, *21*, 387.

(5) (a) Benson, J. W.; Angelici, R. J. *Organometallics* **1992**, *11*, 922. (b) Rao, K. M.; Day, C. L.; Jacobson, R. A.; Angelici, R. J. *Inorg. Chem.* **1991**, *30*, 5046. (c) Choi, M.-G.; Angelici, R. *Organometallics* **1991**, *10*, 2436. (d) Goodrich, J. D.; Nickias, P. N.; Selegue, J. P. *Inorg. Chem.* **1987**, *26*, 3424. (e) Draganjac, M.; Ruffing, C. J.; Rauchfuss, T. B. *Organometallics* **1985**, *4*, 1909. (f) Bucknor, S. M.; Draganjac, M.; Rauchfuss, T. B.; Ruffing, C. J.; Fultz, W. C.; Rheingold, A. L. *J. Am. Chem. Soc.* **1984**, *106*, 5379.

(6) Robertson, M. J.; Day, C. L.; Jacobson, R. A.; Angelici, R. J. *Organometallics* **1994**, *13*, 179.

(7) (a) Ogilvy, A. E.; Skaugset, A. E.; Rauchfuss, T. B. *Organometallics* **1989**, *8*, 2739. (b) Chen, J.; Angelici, R. J. *Organometallics* **1989**, *8*, 2277.

S0276-7333(97)00360-9 CCC: $14.00

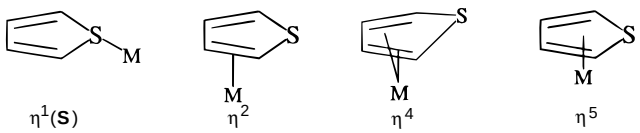

η^1(S) η^2 η^4 η^5

higher nucleophilicities of the thiophene sulfur atoms[10] or they give rise to insertions of the transition metal into C−S bonds.[11] Thiophene adsorption on catalyst surfaces is pertinent; η^1(S) (first observed in (DBT-P(tol)$_2$)$_2$RuCl$_2$ (**2**)[5f] and in [($C_5H_4CH_2C_4H_3S$)Ru(PPh_3)$_2$]-BPh_4 (**3**))[5e] coordination modes are those most frequently reported.[4,12]

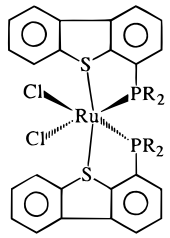

R = p-tolyl
DBT = dibenzothiophene
2

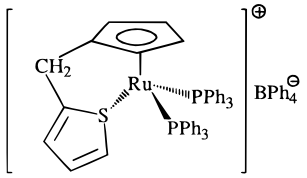

3

The present experimental and theoretical study on ionic interactions of metals with thiophenes centers on the lithiums in $(LiO)_6$ siloxane and alkoxide[13] cores of the X-ray crystal structures of [Li−O−$SiMe_2$(2-C_4H_3S)]$_6$ and [Li−O−CH(*i*-Pr)(2-C_4H_3S)]$_6$, which are applied as electrostatic models for the metals in catalyst surfaces. Computations delineating the Li^+ interactions with thiophene and furan (both σ and π) as well as with SMe_2 and OMe_2 help interpret the experimental findings and provide insight into the "electrostatic component" of metal−thiophene interactions.

Results and Discussion

X-ray Crystal Structures of [Li−O−$SiMe_2$(2-C_4H_3S)]$_6$ (($\mathbf{6}$)$_6$) and [Li−O−CH(*i*-Pr)(2-C_4H_3S)]$_6$ (($\mathbf{9}$)$_6$) and Their Computational Model Systems. While the oxygen analogue of **1-S**, the 2-lithiobenzofuran−tmeda species **1-O**,[3] exhibits short Li−O contacts (Li−O = 2.09(1) Å), no Li−S (Li−S > 3.3 Å) interactions are apparent in **1-S**. In contrast, short Li−S distances are evident in the X-ray crystal structures of the 2-lithio-2-methyl-1,3-dithiane compound **4** (Li−S = 2.516 Å)[14] and in the bis[2-lithiophenyl *tert*-butyl sulfide]−tmeda species **5** (Li−S = 2.712(5) Å).[15]

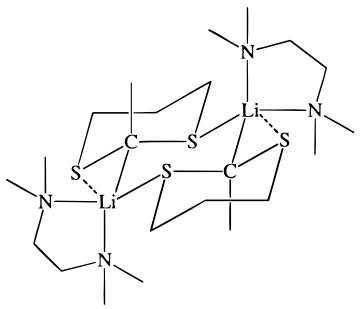

4

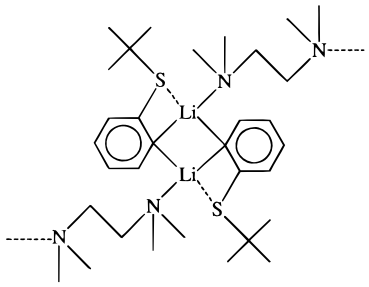

5

Chelation with thiophene ligands results in Ru−S contacts both in **2** and in **3**. To study electrostatic Li−thiophene interactions via the possibility of a five-membered chelate ring, we synthesized and crystallized Li−O−$SiMe_2$(2-C_4H_3S) (**6**).

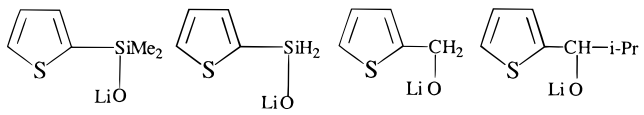

6 **7** **8** **9**

The single-crystal X-ray analysis of **6** reveals the hexameric aggregate [Li−O−$SiMe_2$(2-C_4H_3S)]$_6$ (($\mathbf{6}$)$_6$) (Figure 1). Three different organosilicon fragments comprise the (crystallographic) S_2 structure of ($\mathbf{6}$)$_6$. Two edges of the $(LiO)_6$ cluster, Li_1−O_3 and Li_3−O_1, are capped by two nearly coplanar organosilicon moieties (Li_1−O_3−Si_3−C_{31} = −3.9° and Li_3−O_1−Si_1−C_{11} = 0.2°; Figure 1). The third silicon organic group is aligned between the Li_2−O_2 (Li_2−O_2−Si_2−C_{21} = 40.2°) and Li_{3a}−O_2 bonds (Li_{3a}−O_2−Si_2−C_{21} = −56.1°). The Si_1−R and Si_3−R organic fragments tilt toward Li_3 and Li_1,

(8) (a) Fischer, E. O.; Öfele, K. *Chem. Ber.* **1958**, *91*, 2395. (b) Bailey, M. F.; Dahl, L. F. *Inorg. Chem.* **1965**, *4*, 1306. (c) Sánchez-Delgado, R. A.; Marquez-Silva, R. L.; Puga, J.; Tiripicchio, A.; Tiripicchio-Camellini, M. *J. Organomet. Chem.* **1986**, *316*, C35. (d) Alvarez, M.; Lugan, N.; Donnadieu, B.; Mathieu, R. *Organometallics* **1995**, *14*, 365.

(9) (a) Chen, J.; Young, V. G., Jr.; Angelici, R. J. *Organometallics* **1996**, *15*, 325. (b) Spies, G. H.; Angelici, R. J. *Organometallics* **1987**, *6*, 1897. (c) Lesch, D. A.; Richardson, J. W., Jr.; Jacobson, R. A.; Angelici, R. J. *J. Am. Chem. Soc.* **1984**, *106*, 2901.

(10) (a) Luo, S.; Ogilvy, A. E.; Rauchfuss, T. B.; Rheingold, A. L.; Wilson, S. R. *Organometallics* **1991**, *10*, 1002. (b) Chen, J.; Angelici, R. J. *Organometallics* **1989**, *8*, 2277.

(11) (a) Dullaghan, C. A.; Sun, S.; Carpenter, G. B.; Weldon, B.; Sweigart, D. A. *Angew. Chem.* **1996**, *108*, 234; *Angew. Chem., Int. Ed. Engl.* **1996**, *35*, 212. (b) Myers, A. W.; Jones, W. D. *Organometallics* **1996**, *15*, 2905. (c) Chen, J.; Daniels, L. M.; Angelici, R. J. *Organometallics* **1996**, *15*, 1223. (d) Garcia, J. J.; Mann, B. E.; Adams, H.; Bailey, N. A.; Maitlis, P. M. *J. Am. Chem. Soc.* **1995**, *117*, 2179. (e) Jones, W. D.; Dong, L. *J. Am. Chem. Soc.* **1991**, *113*, 559. (f) Chen, J.; Daniels, L. M.; Angelici, R. J. *J. Am. Chem. Soc.* **1990**, *112*, 199. For C-H activation in thiophenes see: (g) Partridge, M. G.; Field, L. D.; Messerle, B. A. *Organometallics* **1996**, *15*, 872.

(12) Rincón, L.; Terra, J.; Guenzburger, D.; Sánchez-Delgado, R. A. *Organometallics* **1995**, *14*, 1292.

(13) (a) Herrmann, W. A.; Huber, N. W.; Runte, O. *Angew. Chem.* **1995**, *107*, 2371; *Angew. Chem., Int. Ed. Engl.* **1995**, *34*, 2187. (b) Caulton, K. G.; Hubert-Pfalzgraf, L. G. *Chem. Rev.* **1990**, *90*, 969. (c) Veith, M. *Chem. Rev.* **1990**, *90*, 3. (d) Bradley, D. C. *Chem. Rev.* **1989**, *89*, 1317.

(14) Amstutz, R.; Seebach, D.; Seiler, P.; Schweizer, B.; Dunitz, J. D. *Angew. Chem.* **1980**, *92*, 59; *Angew. Chem., Int. Ed. Engl.* **1980**, *19*, 53.

(15) Bauer, W.; Klusener, P.; Harder, S.; Kanters, J. A.; Duisenberg, A. J. M.; Brandsma, L.; Schleyer, P. v. R. *Organometallics* **1988**, *7*, 552.

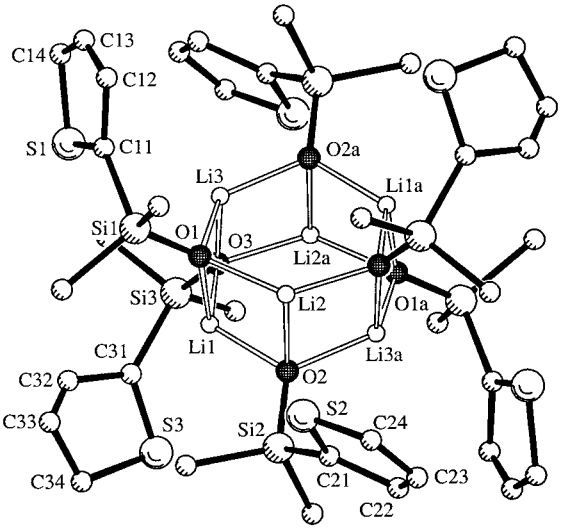

Figure 1. X-ray crystal structure of [Li−O−$SiMe_2$(2-C_4H_3S)]$_6$ ((**6**)$_6$). Hydrogen atoms are omitted.

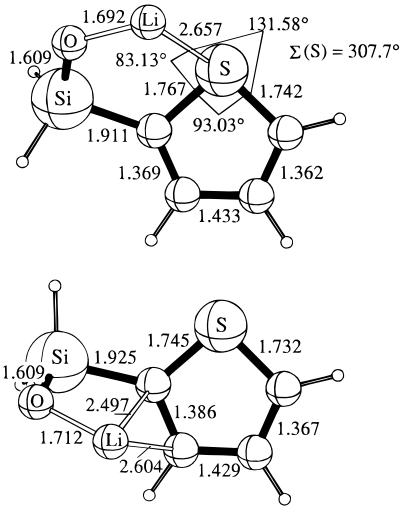

Figure 2. RB3LYP/6-311+G* optimized geometries of Li−O−SiH_2(2-C_4H_3S) with Li−S (**7-S**, C_1) and with Li-C (**7-C**, C_1) coordination modes. Bond lengths are given in Å.

respectively (Li_3−O_1−Si_1 = 111.4°, Li_1−O_3−Si_3 = 111.3°) and result in somewhat different Li−O distances (Li_3−O_1 = 1.970(10) Å, Li_2−O_1 = 1.906(11) Å, Li_1−O_3 = 1.940(10) Å, Li_{2a}−O_3 = 1.905(10) Å). However, the conformations of the thienyl groups preclude Li−S interactions in (**6**)$_6$ (Li_1−S_3 = 3.795(9) Å, Li_3−S_1 = 3.129(9) Å, Li_2−S_2 = 3.364(9) Å); in addition, S_1 and S_2 are only slightly rotated toward Li_3 and Li_2 (S_1−C_{11}−Si_1−O_1 = −65.5°, S_2−C_{21}−Si_2−O_2 = −69.8°), whereas S_3 even is rotated away from Li_1 (S_3−C_{31}−Si_3−O_3 = 103.7°).

As a model system for **6**, monomeric **7** is computed with Li−S (**7-S**; Li−S = 2.657 Å) and with Li−C (**7-C**; Li−C = 2.497, 2.604 Å) contacts (Figure 2). The geometry of **7-C** exhibits a thienyl conformation similar to that in the X-ray crystal structure of (**6**)$_6$. **7-S** is 1.35 kcal/mol more stable than **7-C** (Table 1). The Li−thiophene interactions are expected to increase when the distance between lithium and the thienyl group in **7** is shortened, e.g. by Si/C replacement from **7** to **8**. The Li−S interaction in **8** (Figure 3) is favored slightly more than that in **7**: **8-S** is 1.70 kcal/mol more stable than **8-C** (Table 1), although the preferences are small.

Table 1. Energies of Li−S and Li−C Coordination Modes and Lithium Partial Charges

	total energy (au)[a]	ZPE (NIMAG)[b]	q(Li)[c]	Li−S vs Li−C (kcal/mol)[d]
7-S (C_1)	−926.063 27	49.70 (0)	+0.941	
7-C (C_1)	−926.061 18	49.74 (0)	+0.951	1.35
8-S (C_1)	−674.592 32	55.68 (0)	+0.931	
8-C (C_1)	−674.589 42	55.56 (0)	+0.935	1.70

[a] RB3LYP/6-311+G* optimized geometries. [b] RB3LYP/6-311+G** zero-point energies (ZPE) and number of imaginary frequencies (NIMAG). [c] The natural population analysis was used.[37] [d] Relative energies (including ZPE corrections) of Li−S and Li−C coordination modes.

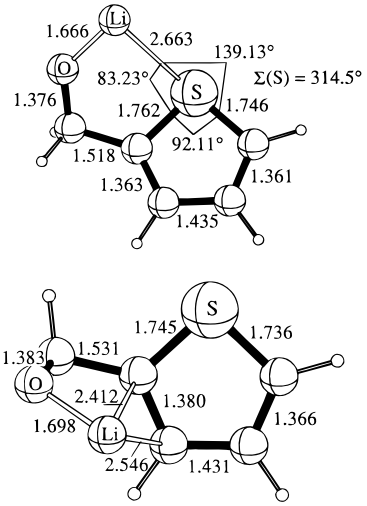

Figure 3. RB3LYP/6-311+G* optimized geometries of Li−O−CH_2(2-C_4H_3S) with Li−S (**8-S**, C_1) and with Li-C (**8-C**, C_1) coordination modes. Bond lengths are given in Å.

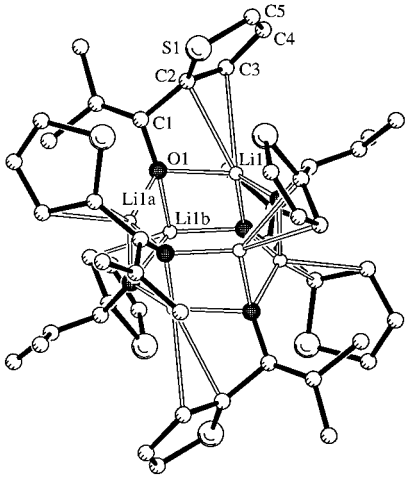

Figure 4. X-ray crystal structure of [Li−O−CH(*i*-Pr)(2-C_4H_3S)]$_6$ ()**9**)$_6$). Hydrogen atoms are omitted.

As the experimental equivalent of **8**, Li−O−CH(*i*-Pr)-(2-C_4H_3S) (**9**) was synthesized and crystallized. Relative to **6**, increased Li−thiophene interactions are structurally apparent in **9** (as they are above between **7** and **8**). The single-crystal X-ray structure of the hexameric S_6 symmetrical (crystallographic) aggregate (**9**)$_6$ (Figure 4) shows the C_1−C_2 bonds to be aligned in about the same plane as the Li_1−O_1 edge of the (LiO)$_6$ cluster (Li_1−O_1−C_1−C_2 = 9.8°; Figure 4). The organic fragments tilt toward Li_1 (Li_1−O_1−C_1 = 111.0(4)°, Li_{1a}−O_1−C_1 = 115.7(5)°), and the Li−O distances are different (Li_1−O_1 = 1.940(8) Å, Li_{1a}−O_1 = 1.874(7) Å, Li_{1b}−O_1 = 1.923(7) Å). As in (**6**)$_6$, Li−S contacts would be expected

Chart 1. Thienyl (E_1 = S) and Furanyl (E_1 = O) Rotations

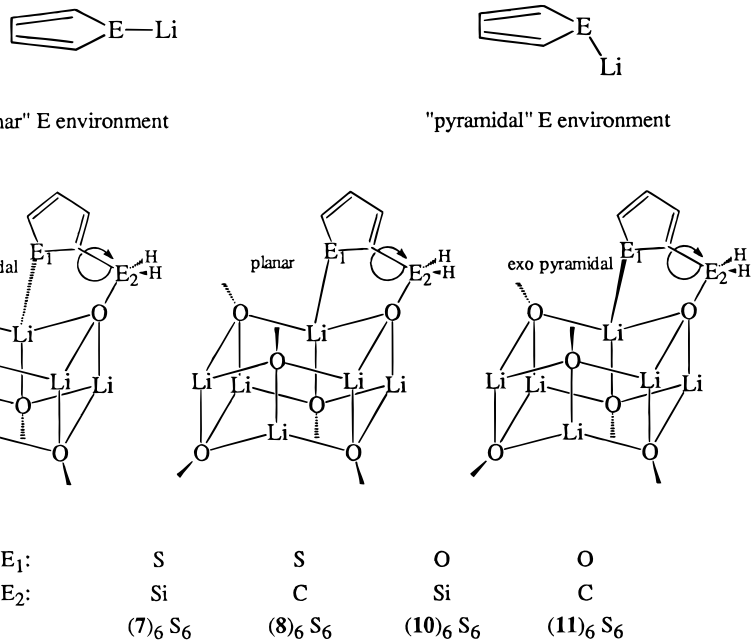

E_1:	S	S	O	O
E_2:	Si	C	Si	C
	$(7)_6$ S_6	$(8)_6$ S_6	$(10)_6$ S_6	$(11)_6$ S_6

if the thienyl groups were rotated around the C_1-C_2 bond in $(9)_6$, but such Li−S interactions are avoided again (Li_1-S_1 = 3.614(9) Å). The conformations of the 2-thienyl groups in $(9)_6$ ($S_1-C_2-C_1-O_1 = -116.3°$, $C_3-C_2-C_1-O_1 = 61.0°$) resemble those of the computational model **8-C**, and short Li−C contacts (Li_1-C_2 = 2.631(7) Å, Li_1-C_3 = 2.845(7) Å) are apparent in $(9)_6$.

The $(LiO)_6$ cores of the X-ray crystal structures $(6)_6$ and $(9)_6$ are modeled only poorly by the monomeric Li−O units of **7** and **8**; hence, we examined Li−thiophene interactions in hexameric $(7)_6$ and $(8)_6$ by the semiempirical PM3[16] method. The conformational analyses of the thienyl rotations on the $(LiO)_6$ cores reveal two minima for both $(7)_6$ and $(8)_6$ with short "pyramidal"[17] endo and exo Li−S(thiophene) contacts (Chart 1, Figures 5 and 6). Such Li−S interactions are not observed experimentally in $(6)_6$ and $(9)_6$.[18] Both $(7)_6$-**endo** and $(8)_6$-**endo** are slightly more stable than $(7)_6$-**exo** and $(8)_6$-**exo** (Chart 1, Figures 5 and 6). Planar[17] Li−S(thiophene) coordination modes correspond to the thienyl rotation transition structures $(7)_6$-**TS** and $(8)_6$-**TS** (Chart 1, Figures 5 and 6).

Comparisons between $(7)_6$ and $(8)_6$ and their oxygen analogues $(10)_6$ and $(11)_6$ are intriguing, as the dipole moments in thiophene and furan have similar magnitudes and the same directions (Table 2).[19] However, the conformational analyses for the furan systems $(10)_6$ and $(11)_6$ (Figures 7 and 8) differ significantly from the thienyl rotation data in $(7)_6$ and $(8)_6$: while the planar Li−S coordination modes in $(7)_6$ and in $(8)_6$ correspond to transition structures of the thienyl rotations on the $(LiO)_6$ cores (Figures 5 and 6), both $(10)_6$ and $(11)_6$ are minima with planar Li−O contacts (Figures 7 and 8).

Lithio-Aversion of the Sulfur Atoms in Thiophene. Why are Li−S(thiophene) interactions avoided in the X-ray crystal structures of both $(6)_6$ and $(9)_6$? Why is a Li−(C=C) interaction preferred in $(9)_6$ instead? Since the dipole moments (both negative at the heteroatom) of thiophene **12** (0.547 D) and of furan **13** (0.734 D; Table 2)[19] are similar, what is responsible for the puzzling differences in Li^+ coordinations to the thiophene vs the furan moieties in **1-S** and **1-O** as well as in $(7)_6$, $(8)_6$, and $(10)_6$ and $(11)_6$?

The σ-"in-plane" Li^+ coordination energy to thiophene (**12-σ**, 16.9 kcal/mol) is considerably less than that to furan (**13-σ**, 29.2 kcal/mol, Chart 2, Table 3, Figure 9). However, the π Li^+ coordination energy in **12-π** (32.1 kcal/mol) is higher than in **13-π** (29.6 kcal/mol; Chart 2, Table 3, Figure 9).[13−20] While $E_{coord}(Li^+)$ values are similar in **13-σ** and in π ($\Delta_{\sigma-\pi}[E_{coord}(Li^+)] = -0.3$ kcal/mol), they are in **12-π** much higher than in **12-σ** ($\Delta_{\sigma-\pi}[E_{coord}(Li^+)] = -15.2$ kcal/mol, Table 3); this is consistent with the lithio-aversion of the thiophene sulfur atoms in the X-ray crystal structures of $(6)_6$ and $(9)_6$.

E = S	**12-σ** (C_{2v})	E = S	**12-π** (C_s)
E = O	**13-σ** (C_{2v})	E = O	**13-π** (C_s)
E = P^-	**14-σ** (C_{2v})	E = P^-	**14-π** (C_s)
E = N^-	**15-σ** (C_{2v})	E = N^-	**15-π** (C_s)

Alkali-metal η^5 π-coordinations to the isoelectronic phospholide $C_4H_4P^-$ (**14**)[21] and pyrrolide $C_4H_4N^-$ (**15**)

(16) (a) Stewart, J. J. P. *J. Comput. Chem.* **1989**, *10*, 209. Li parameters: (b) Anders, E.; Koch, R.; Freunscht, P. *J. Comput. Chem.* **1993**, *14*, 1301.

(17) Pyramidal M−S(thiophene) coordination is found exclusively in transition-metal thiophene complexes rather than the planar M−S(thiophene) mode; see ref 4 and literature cited therein.

(18) The overestimation of "agostic" H−Li interactions by the PM3 method is known: Opitz, A.; Koch, R.; Katritzky, A. R.; Fan, W. Q.; Anders, E. *J. Org. Chem.* **1995**, *60*, 3743.

(19) Barton, T. J.; Roth, R. W.; Verkade, J. G. *J. Am. Chem. Soc.* **1972**, *94*, 8854.

(20) The experimental proton affinity of thiophene (195.8 kcal/mol) is 3.6 kcal/mol greater than that of furan (192.2 kcal/mol). In both cases, the protons are attached to the C_α-sites rather than to the C_β or heteroatom sites. However, this reflects primarily the greater stability in the covalently bound ions: (a) Lias, S. G.; Liebman, J. F.; Levin, R. D. *J. Phys. Chem. Ref. Data* **1984**, *13*, 695. (b) Lias, S. G.; Bartmess, J. E.; Liebman, J. F.; Holmes, J. L.; Levin, R. D.; Mallard, W. G. *J. Phys. Chem. Ref. Data* **1988**, *17*, 146. (c) Houriet, R.; Schwarz, H.; Zummack, W.; Andrade, J. G.; Schleyer, P. v. R. *Nouv. J. Chim.* **1991**, *5*, 505.

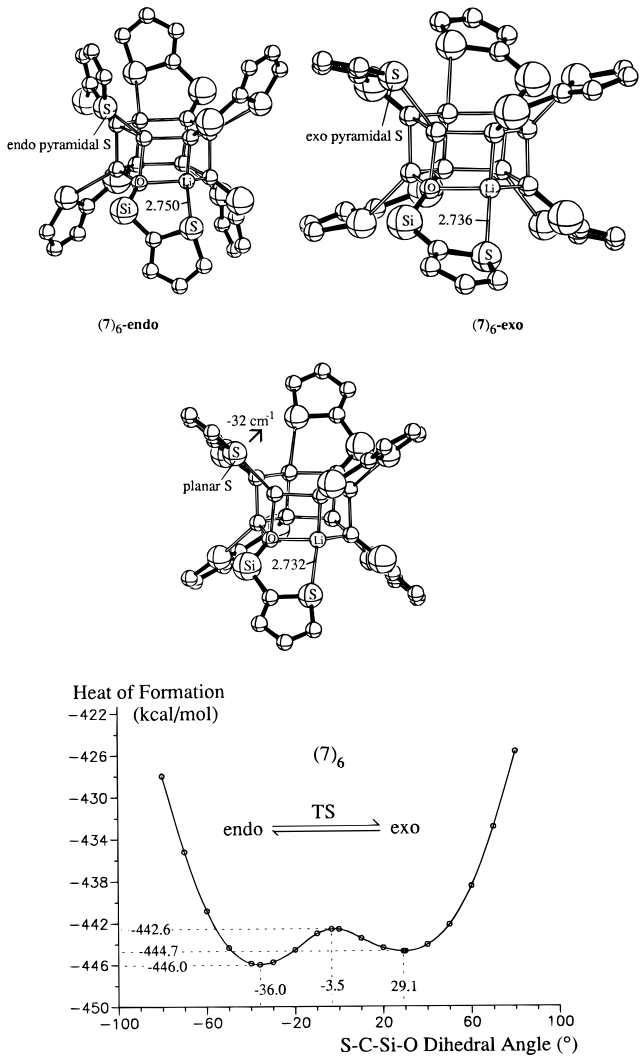

Figure 5. (a, top) PM3 optimized geometries of $[Li-O-SiH_2(2\text{-}C_4H_3S)]_6$ ((**7**)$_6$). Bond lengths are given in Å. (b, bottom) PM3 conformational analysis of the thienyl rotations on the $(LiO)_6$ core of $[Li-O-SiH_2(2\text{-}C_4H_3S)]_6$ ((**7**)$_6$).

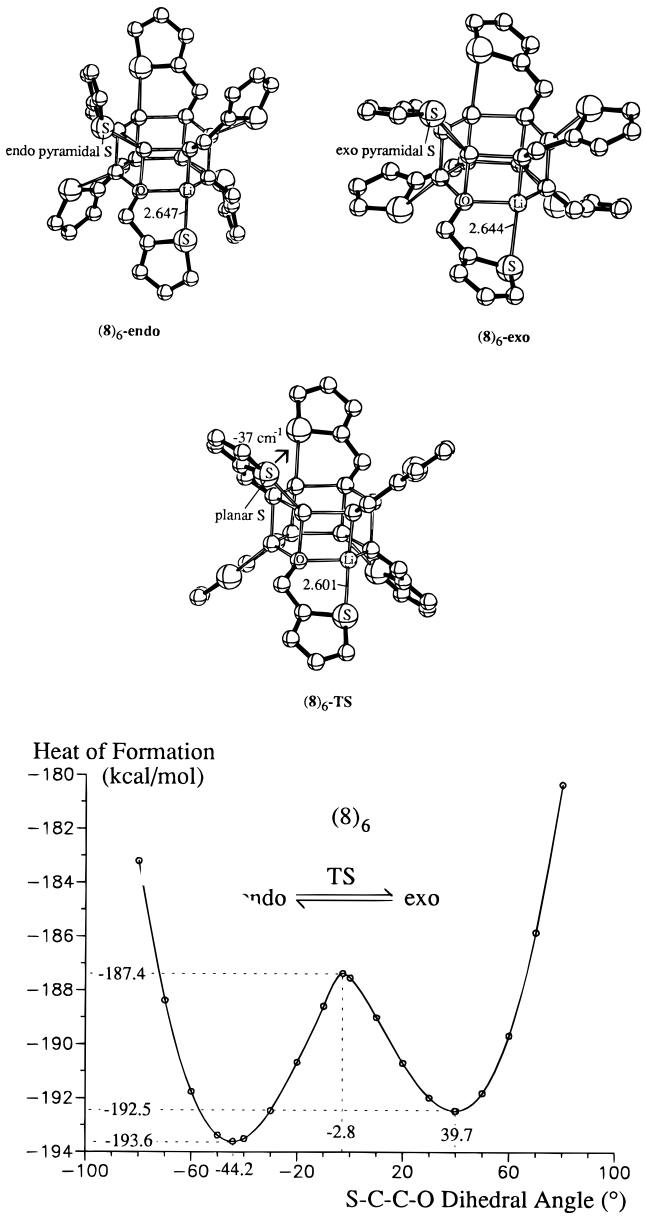

Figure 6. (a, top) PM3 optimized geometries of $[Li-O-CH_2(2\text{-}C_4H_3S)]_6$ ((**8**)$_6$). Bond lengths are given in Å. (b, bottom) PM3 conformational analysis of the thienyl rotations on the $(LiO)_6$ core of $[Li-O-CH_2(2\text{-}C_4H_3S)]_6$ ((**8**)$_6$).

anions are found frequently.[22] Earlier computations on lithium pyrrolide C_4H_4NLi showed **15-*π*** to be more stable than **15-*σ***.[23] The X-ray crystal structures of lithium indolide,[24] sodium indolide,[24] potassium carbazolide,[25] and cesium carbazolide[25] point to an increasing preference for alkali-metal π-interactions with increasing ion size. Our computations also show that Li^+ π-coordinated isomers are favored over the in-plane σ-alternatives for both **15** and **14** (Table 3). Why is the Li^+ π-interaction preference so much larger for **12** (S) and for **14** (P^-) than for the second-row congeners **13** (O) and **15** (N^-) (Table 3, Figure 9)?

Aromaticity (cyclic delocalization) might be responsible. Delocalization of the p lone pairs of the heteroatoms E results in decreased σ(E)- and increased π-affinity to the Li^+ ions, as illustrated by resonance contributions:[26]

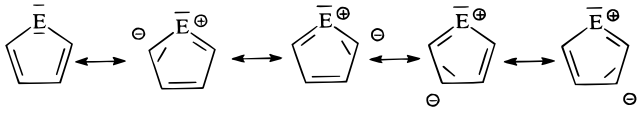

Consistent with the aromatic delocalization in **12**, the σ-in-plane Li^+ affinity of thiophene in **12-*σ***, 16.9 kcal/

(21) (a) Paul, F.; Carmichael, D.; Ricard, L.; Mathey, F. *Angew. Chem.* **1996**, *108*, 1204; *Angew. Chem., Int. Ed. Engl.* **1996**, *35*, 1125. (b) Mathey, F. *Chem. Rev.* **1988**, *88*, 429.

(22) For η^5 coordinations in silole mono- and dianions see: (a) Goldfuss, B.; Schleyer, P. v. R. *Organometallics* **1995**, *14*, 1553. (b) Goldfuss, B.; Schleyer, P. v. R.; Hampel, F. *Organometallics* **1996**, *15*, 1755. (c) Goldfuss, B.; Schleyer, P. v. R. *Organometallics* **1997**, *16*, 1543. (d) Freeman, W. P.; Tilley, T. D.; Rheingold, A. L. *J. Am. Chem. Soc.* **1994**, *116*, 8428. (e) West, R.; Sohn, H.; Bankwitz, U.; Calabrese, J.; Apeloig, Y.; Müller, T. *J. Am. Chem. Soc.* **1995**, *117*, 11608. (f) Freeman, W. P.; Tilley, T. D.; Yap, G. P. A. *Angew. Chem.* **1996**, *108*, 960; *Angew. Chem., Int. Ed. Engl.* **1996**, *35*, 882. For η^5-coordinated germole anions see: (g) West, R.; Sohn, H.; Powell, D. R.; Müller, T. Apeloig, Y. *Angew. Chem.* **1996**, *108*, 1095; *Angew. Chem., Int. Ed. Engl.* **1996**, *35*, 1002. (h) Hong, J.-H.; Pan, Y.; Boudjouk, P. *Angew. Chem.* **1996**, *35*, 213; *Angew. Chem., Int. Ed. Engl.* **1996**, *35*, 186.

(23) Hacker, R.; Kaufmann, E.; Schleyer, P. v. R.; Mahdi, W.; Dietrich, H. *Chem. Ber.* **1987**, *120*, 1533.

(24) Gregory, K.; Bremer, M.; Bauer, W.; Schleyer, P. v. R. *Organometallics* **1990**, *9*, 1485.

(25) Gregory, K.; Bremer, M.; Schleyer, P. v. R.; Klusener, P. A. A.; Brandsma, L. *Angew. Chem.* **1989**, *101*, 1261; *Angew. Chem., Int. Ed. Engl.* **1989**, *28*, 1224.

(26) For an alternative description see: Laidig, K. E.; Speers, P.; Streitwieser, A. *Can. J. Chem.* **1996**, *74*, 1215.

Table 2. Atomic Charges (au) and Dipole Moments (D) of Thiophene (C_{2v}, 12) and Furan (C_{2v}, 13)

	E	C_α	C_β	H(C_α)	H(C_β)	dipole moment[b]
			12, E = S			
						0.547,[a] 0.52,[c] 0.55[d]
NPA[a,e]	+0.447	−0.453	−0.287	+0.265	+0.252	
Mulliken[a,f]	+0.114	−0.313	−0.151	+0.218	+0.189	
MK[a,g]	+0.039	−0.217	−0.134	+0.191	+0.141	
CHelpG[a,h]	+0.017	−0.193	−0.065	+0.161	+0.088	
PM3[i]	+0.304	−0.300	−0.122	+0.146	+0.124	0.674
			13, E = O			
						0.734,[a] 0.71,[c] 0.66[d]
NPA[a,e]	−0.464	+0.086	−0.340	+0.233	+0.254	
Mulliken[a,f]	−0.252	−0.132	−0.131	+0.197	+0.192	
MK[a,g]	−0.187	+0.015	−0.215	+0.133	+0.161	
CHelpG[a,h]	−0.180	+0.002	−0.135	+0.115	+0.108	
PM3[i]	−0.067	−0.066	−0.179	+0.147	+0.132	0.216

[a] RB3LYP/6-31+G* optimized geometries and wave functions. [b] In both **12** and **13**, the negative ends of the electrical dipole vectors are at the heteroatom (for an experimental evaluation of the direction of the dipole moment, see ref 19). [c] Experimental measurement in benzene solution at 25 °C; see ref 19 and literature cited therein. [d] Experimental gas phase measurement.[36] [e] Natural population analysis.[37] [f] Mulliken charges.[38] [g] Electrostatic potential derived Merz−Kollman−Singh charges.[39] [h] CHelpG electrostatic potential-derived charges.[40] [i] Semiempirical PM3 method.[16]

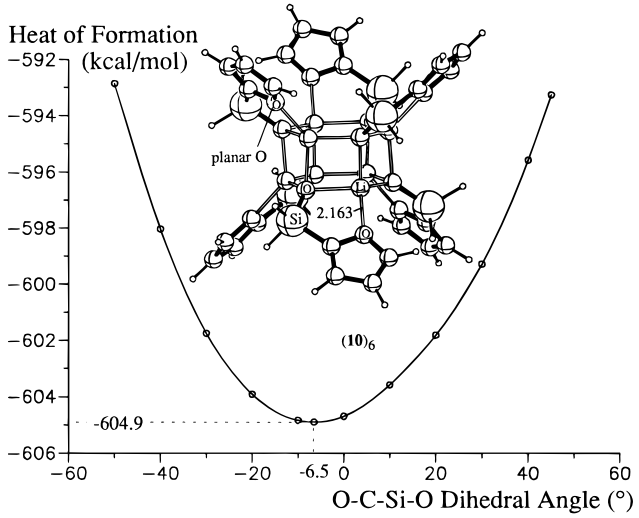

Figure 7. PM3 conformational analysis of the furanyl rotations on the $(LiO)_6$ core of $[Li{-}O{-}SiH_2(2\text{-}C_4H_3O)]_6$ ($(\mathbf{10})_6$). The most stable geometry" is shown.

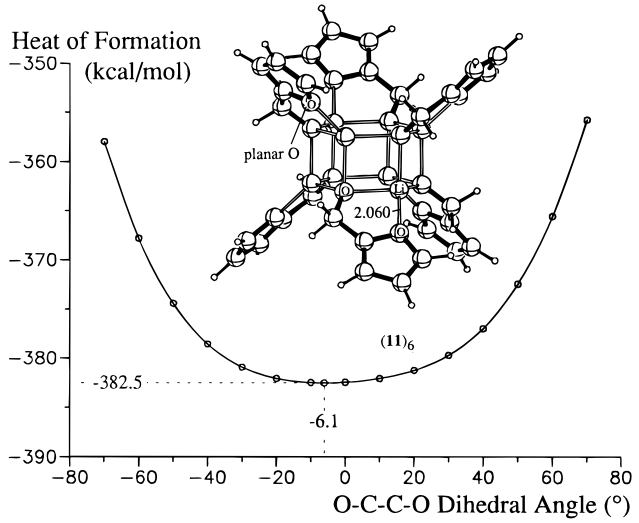

Figure 8. PM3 conformational analysis of the furanyl rotations on the $(LiO)_6$ core of $[Li{-}O{-}CH_2(2\text{-}C_4H_3O)]_6$ ($(\mathbf{11})_6$). The most stable geometry is shown.

mol, is reduced by 12.6 kcal/mol (Table 4) relative to that of the nonaromatic reference $Li^+{-}SMe_2$ (**16-Li*C*$_{2v}$**, $E_{coord}(Li^+)$ = 29.5 kcal/mol; Chart 2, Table 3, Figure 10).

Chart 2. Comparison of Li^+ Binding Energies (kcal/mol)

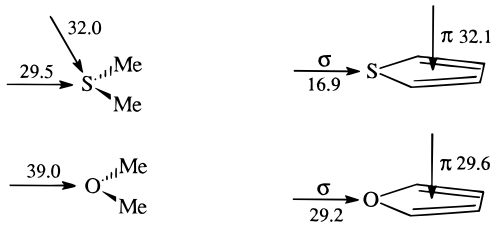

The greater aromaticity of thiophene (**12**) relative to that of furan (**13**) is apparent from structural, energetic, and magnetic criteria (see Table 4).[27,28] Due to the smaller aromaticity of furan (**13**), the Li^+ σ-in-plane coordination energy in **13-*σ*** ($E_{coord}(Li^+)$ = 29.2 kcal/mol) is reduced by 9.8 kcal/mol (Table 4, Chart 2) relative to the $Li^+{-}OMe_2$ reference **17-*C*$_{2v}$** ($E_{coord}(Li^+)$ = 39.0 kcal/mol). This reduction is 2.8 kcal/mol smaller than that for thiophene (Table 4). Remarkably, this 2.8 kcal/mol difference in the Li^+ σ-in-plane" E_{coord} values of **12** and **13** is nearly the same as the difference in the aromatic stabilization energies (ΔASE = 2.6 kcal/mol) of **12** (ASE = 22.4 kcal/mol) and **13** (ASE = 19.8 kcal/mol, Table 4). The $E_{coord}(\pi\text{-}Li^+)$ value is 2.5 kcal/mol greater for thiophene in **12-*π*** (32.1 kcal/mol) than for furan in **13-*π*** (29.6 kcal/mol, Chart 2). This is consistent with the reduced Li^+ σ-in-plane E_{coord} value (2.8 kcal/mol) and the relative ASE (2.6 kcal/mol) of **12** and **13** (Table 4, Chart 2).

As for the Li^+ complexes, the relative coordination energies of the LiOH complexes $HOLi{-}SC_4H_4$ (**12-*σ*** C_{2v}, **12-*π*OH** C_s, corresponding to **12*σ*,*π***) and $HOLi{-}OC_4H_4$ (**13-*σ*** C_{2v}, **13-*π*OH** C_s, corresponding to **13*σ*,*π***) show preferences for out-of-plane π-coordination for E = S in **12-*π*OH** and for in-plane heteroatom coordination for E = O in **13-*σ*OH** (Table 3). The positive lithium charges near unity in thiophene and furan complexes point to the electrostatic nature of the interactions (see NPA charges in Tables 1 and 3).

Electrostatic potential (EP) patterns provide useful descriptions of Li^+ coordination sites in organic mol-

(27) Schleyer, P. v. R.; Freeman, P. K.; Jiao, H.; Goldfuss, B. *Angew. Chem.* **1995**, *107*, 332; *Angew. Chem., Int. Ed. Engl.* **1995**, *34*, 337.
(28) Schleyer, P. v. R.; Maerker, C.; Dransfeld, A.; Jiao, H.; Hommes, N. J. R. v. E. *J. Am. Chem. Soc.* **1996**, *118*, 6317.

Table 3. Lithium Coordination Energies and Lithium Partial Charges[a]

	total energies (au)	ZPE (kcal/mol)[b]	E_{coord}(Li) (kcal/mol)[c]	q(Li)[d]	$\Delta_{\sigma-\pi}[E_{coord}(Li)]$ (kcal/mol)[c]
12 (C_{2v})	−553.073 16	37.60 (0)			
12-σ (C_{2v})	−560.390 20	40.84 (1)	16.92	+0.962	
12-π (C_s)	−560.415 39	41.47 (0)	32.09	+0.943	−15.2
12-σOH (C_{2v})	−636.498 02	47.95 (2)[e]	1.79	+0.937	
12-πOH (C_s)	−636.505 46	48.15 (0)	6.25	+0.940	−4.5
13 (C_{2v})	−230.087 85	42.29(0)			
13-σ (C_{2v})	−237.420 53	43.02 (0)	29.24	+0.985	
13-π (C_s)	−237.421 55	43.34 (0)	29.56	+0.959	−0.3
13-σOH (C_{2v})	−313.524 18	50.29 (1)[e]	11.33	+0.950	
13-πOH (C_s)	−313.518 77	50.16 (0)	8.07	+0.946	+3.3
14 (C_{2v})	−496.267 36	38.77 (0)			
14-σ (C_{2v})	−503.759 59	40.27 (1)	128.59	+0.876	
14-π (C_s)	−503.807 58	41.18 (0)	157.79	+0.905	−29.2
15 (C_{2v})	−209.645 68	40.89 (0)			
15-σ (C_{2v})	−217.173 37	42.77 (0)	150.46	+0.953	
15-π (C_s)	−217.190 37	43.55 (0)	160.35	+0.922	−9.9
16 (C_{2v})	−478.066 69	47.27 (0)[f]			
16-LiC_{2v} (C_{2v})	−485.400 37	48.35 (1)[f]	29.52	+0.949	
16-LiC_s (C_s)	−485.404 68	48.53 (0)[f]	32.04	+0.933	−2.5
17 (C_{2v})	−155.077 04	49.73 (0)[f]			
17-LiC_{2v} (C_{2v})	−162.426 73	51.34 (0)[f]	39.03	+0.979	

[a] RB3LYP/6-311+G** optimized geometries. [b] RHF/6-31G* zero-point energies (scaled by 0.89);[42] number of imaginary frequencies (NIMAG) in parentheses. [c] Including ZPE corrections: Li^+ (B3LYP/6-311+G*), −7.284 92 au; LiOH ($C_{\infty v}$, (B3LYP/6-311+G**), −83.417 33 au; ZPE, 7.41 kcal/mol; NIMAG = 0. [d] The natural population analysis was used.[37] [e] The most negative frequency corresponds to an in-plane motion of the HOLi moiety. [f] RB3LYP/6-311+G** frequency calculations.

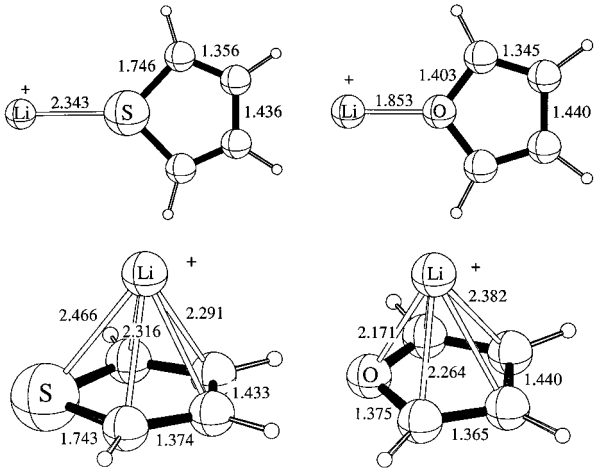

Figure 9. RB3LYP/6-311+G** optimized geometries of σ-Li^+−C_4H_4S (**12-σ**, C_{2v}), π-Li^+−C_4H_4S (**12-π**, C_s), σ-Li^+−C_4H_4O (**13-σ**, C_{2v}), and π-Li^+−C_4H_4O (**13-π**, C_s). Bond lengths are given in Å.

Table 4. $E_{coord}(Li^+)$ and Aromaticity Criteria

	12	(**12**−**13**)	**13**
ASE (kcal/mol)[a]	22.4	2.6	19.8
$E_{coord}(Li^+)$ (kcal/mol)			
σ[b]	16.9	−12.3	29.2
σ-EMe_2[c]	−12.6	−2.8	−9.8
π[b]	32.1	2.5	29.6
NICS (ppm)[d]	−13.6	−1.3	−12.3

[a] RMP2(fc)/6-31G* aromatic stabilization energies.[27] [b] Li^+-π- and σ-in-plane coordination energies (Table 3). [c] Differences between the σ-in-plane and the EMe_2 Li^+ coordination energies (Table 3). [d] Nucleus-independent chemical shifts.[28]

ecules.[1] Thus, the sulfur atom in **12** is positively charged, whereas the oxygen in **13** is negatively charged according to a variety of population analyses (Table 2). Second-period elements exhibit generally higher electronegativities than their heavier congeners.[29] Consequently, the slightly negative in-plane EP pattern in **12** (Figure 11a) reflects the low Li^+ affinity at the sulfur atom, whereas in **13**, a strongly negative EP at oxygen is apparent (Figure 11a). Similarly, the out-of-plane EP map of **13** (Figure 11b) shows the most negative contribution in the ring plane near oxygen. In contrast, the EP of **12** is more negative atom above the ring plane than in the plane near the sulfur (Figure 11b).

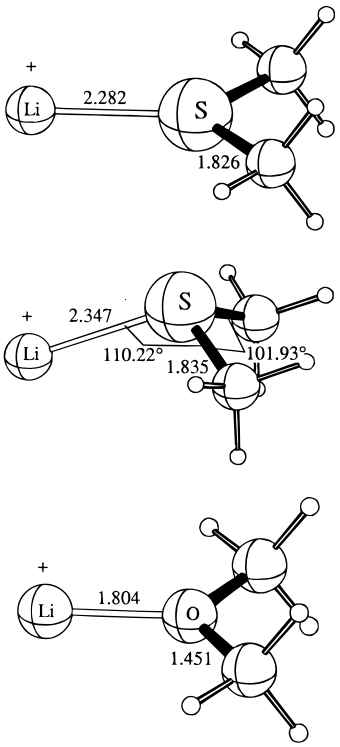

Figure 10. RB3LYP/6-311+G** optimized geometries of Li^+−SMe_2 (**16-LiC_{2v}**, C_{2v}; **16-LiC_s**, C_s), and of Li^+−OMe_2 (**17-LiC_{2v}**, C_{2v}). Bond lengths are given in Å.

The methyl derivatives **16** and **17** provide even more detailed EP analyses at the heteroatoms: whereas the favorable Li^+ locations in **16** are indicated by "rabbit ear" shaped EP depressions at sulfur, a single EP

(29) Bergmann, D.; Hinze, J. *Angew. Chem.* **1996**, *108*, 162; *Angew. Chem., Int. Ed. Engl.* **1996**, *35*, 150 and references therein.

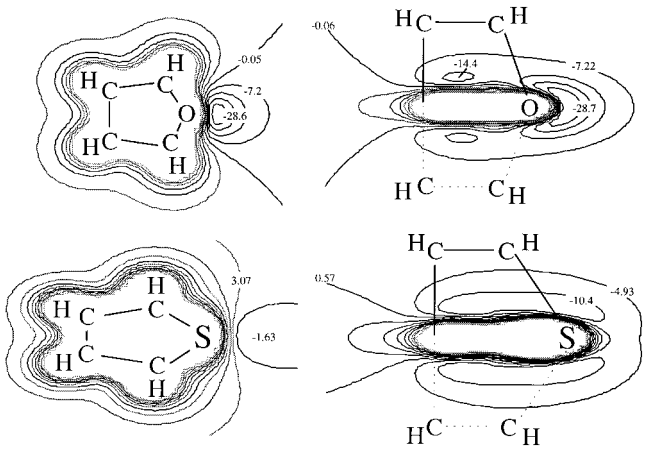

Figure 11. (a, top) In-plane electrostatic potential maps (kcal/mol) of furan (**13**, C_{2v}) and thiophene (**12**, C_{2v}) (RHF/6-31+G*//RB3LYP/6-31+G*). (b, bottom) Out-of-plane electrostatic potential maps (kcal/mol) of furan (**13**, C_{2v}) and thiophene (**12**, C_{2v}) (RHF/6-31+G*//RB3LYP/6-31+G*).

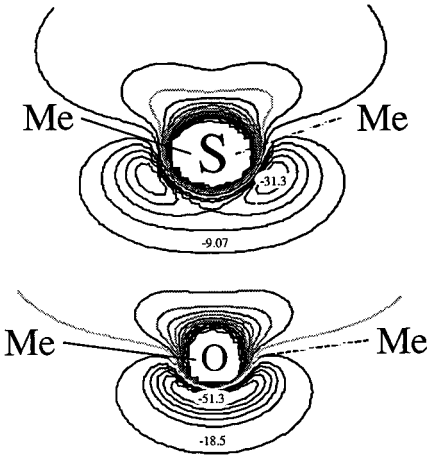

Figure 12. Electrostatic potential maps (kcal/mol) of SMe_2 (**16**, C_{2v}) and OMe_2 (**17**, C_{2v}) (RHF/6-31+G*//RB3LYP/6-31+G*).

minimum is shown in front of oxygen in **17** (Figure 12). This is consistent with the pyramidal S and the planar O orientations in **16-LiC_s** and in **17-LiC_{2v}** (Figure 10).

The different in-plane EPs of **12** and of **13** are clearly apparent even at distances of 2 Å from the heteroatoms: the oxygen atom in **13** has one strongly negative EP depression (Figure 13a), but two slightly negative potential minima—separated by a saddle point—are seen in **12** (Figure 13b). In contrast, the π-contributions of the EPs 2 Å from the ring planes are very similar for **13** (Figure 14a) and for **12** (Figure 14a).

Hence, electrostatic potentials nicely reflect the lithio-aversion of the sulfur atom in thiophene (**12**). This is clearly evident energetically as well (Table 3). The only slightly negative in-plane EP of **12** discourages Li^+−S coordination in **12-σ** in competition with the Li^+ π-interaction in **12-π**. The latter is supported strongly by the negative out-of-plane EP of **12**. Hence, possible Li−S coordinations are avoided in the X-ray crystal structures of $(\mathbf{6})_6$ and of $(\mathbf{9})_6$ and Li−(C=C) π-interactions are favored in $(\mathbf{9})_6$ instead.

Conclusions

No short contacts between the lithiums in the $(LiO)_6$ cores and the thiophene sulfur atoms are found in the X-ray crystal structures of $[Li-O-SiMe_2(2\text{-}C_4H_3S)]_6$ $(\mathbf{6})_6$ and of $[Li-O-CH(i\text{-}Pr)(2\text{-}C_4H_3S)]_6$ $(\mathbf{9})_6$ (Li−S > 3 Å). Instead, Li−(C=C) π-interactions ($Li_1-C_2 = 2.631(7)$ Å, $Li_1-C_3 = 2.845(7)$ Å) are apparent in $(\mathbf{9})_6$.

The monomeric computational models $Li-O-SiH_2(2\text{-}C_4H_3S)$ (**7**) and $Li-O-CH_2(2\text{-}C_4H_3S)$ (**8**) favor slightly (1.4 and 1.7 kcal/mol) Li−S over Li−(C=C) contacts. The PM3 analyses of thienyl group conformations on the $(LiO)_6$ cores in $[Li-O-SiH_2(2\text{-}C_4H_3S)]_6$ $((\mathbf{7})_6)$ and in $[Li-O-CH_2(2\text{-}C_4H_3S)]_6$ $((\mathbf{8})_6)$ show preference for pyramidal Li−S(thiophene) environments, whereas the furanyl groups in $[Li-O-SiH_2(2\text{-}C_4H_3O)]_6$ $((\mathbf{10})_6)$ and $[Li-O-CH_2(2\text{-}C_4H_3O)]_6$ $((\mathbf{11})_6)$ favor planar Li−O(furan) interactions. Decreased σ- and increased π-Li^+ coordination energies of thiophene (**12**) relative to furan (**13**) are consistent with the greater aromaticity of **12**. The basic difference (brought out in Chart 2) is that Li^+ coordination strongly prefers π- over σ-modes for thiophene (**12**), but the complexation energies at both sites are nearly the same for furan (**13**).

Electrostatic potential (EP) analyses show considerably smaller negative contributions in the ring plane of thiophene (**12**) at sulfur than in the out-of-plane π-region. In contrast, furan (**13**) exhibits the most negative EP at oxygen in the ring plane. Consequently, the Li^+−S(thiophene) coordination in **12-σ** is strongly disfavored relative to the π-contact in **12-π**. Hence, the lack of Li−S interactions in the X-ray crystal structures of $(\mathbf{6})_6$ and of $(\mathbf{9})_6$ reflects structural consequences of the lithio-aversion of thiophene sulfur atoms. Electrostatic metal-thiophene interactions prefer the thiophene π-system rather than the in-plane region at the sulfur atom.

Experimental Section

The experiments were carried out under an argon atmosphere by using standard Schlenk as well as needle/septum techniques. The solvents were freshly distilled from sodium/benzophenone under argon. Thiophene, dichlorodimethylsilane, and isobutyraldehyde (Acros) were distilled prior to use. The NMR spectra were recorded on JEOL GX and JEOL Alpha 500 (CP-MAS) spectrometers (^{1}H, 400 MHz; ^{13}C, 100.6 MHz) and referenced to TMS or to adamantane (CP-MAS). IR spectra were determined as neat samples or as Nujol mulls between NaCl disks on a Perkin-Elmer 1420 spectrometer. Mass spectral data were obtained on a Varian MAT 311A spectrometer and the elemental analyses (C, H) on a Heraeus Micro Automaton. The X-ray crystal data were collected with a Siemens P4 diffractometer using the ω/θ-scan method. The structures were solved by direct methods using SHELXTL Plus 4.11. The parameters were refined, with all data by full-matrix least squares on F^2 using SHELXL93 (G. M. Sheldrick, Göttingen, Germany, 1993). All non-hydrogen atoms were refined anisotropically; the hydrogen atoms were fixed in idealized positions using a riding model. $R1 = \sum|F_o - F_c|/\sum F_o$ and $\sum wR2 = \sum w|(F_o^2 - F_c^2)^2|/\sum(w(F_o^2)^2)^{0.5}$. Further details are available on request from the Director of the Cambridge Crystallographic Data Center, Lensfield Road, GB-Cambridge CB2 1 EW, U.K., by quoting the journal citation.

Li−O−SiMe$_2$(2-C$_4$H$_3$S) (6). A solution of 5.4 g (0.06 mol) of 2-lithiothiophene in THF/hexane was prepared from 37.5 mL (0.06 mol) of *n*-BuLi (1.6 M in hexane) and 6.05 g (0.072 mol) of thiophene in 50 mL of THF.[30] This solution was added dropwise at 0 °C to 7.7 g (0.06 mol) of dichlorodimethylsilane in 150 mL of diethyl ether. After the resulting mixture was stirred at room temperature for 3 h, the suspension was

(30) Brandsma, L.: Verkruijsse, H. *Preparative Polar Organometallic Chemistry*; Springer: Berlin, 1987.

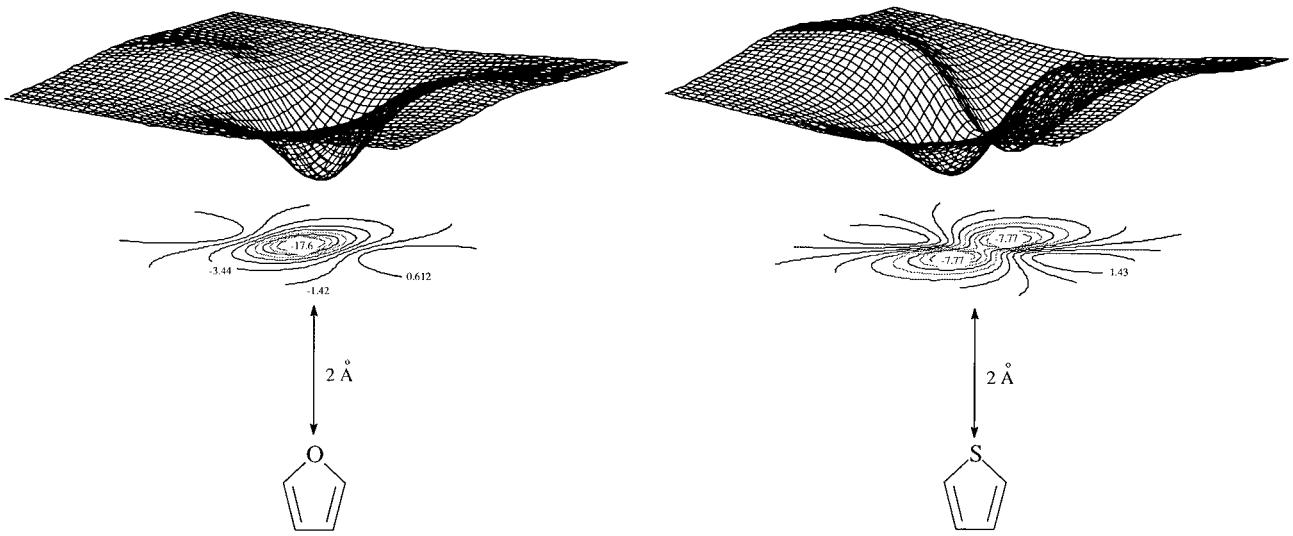

Figure 13. In-plane electrostatic potential surfaces and maps (kcal/mol) 2 Å from (a, top) the furan (**13**, C_{2v}) oxygen atom (RHF/6-31+G*//RB3LYP/6-31+G*) and (b, bottom) the thiophene (**12**, C_{2v}) sulfur atom (RHF/6-31+G*//RB3LYP/6-31+G*).

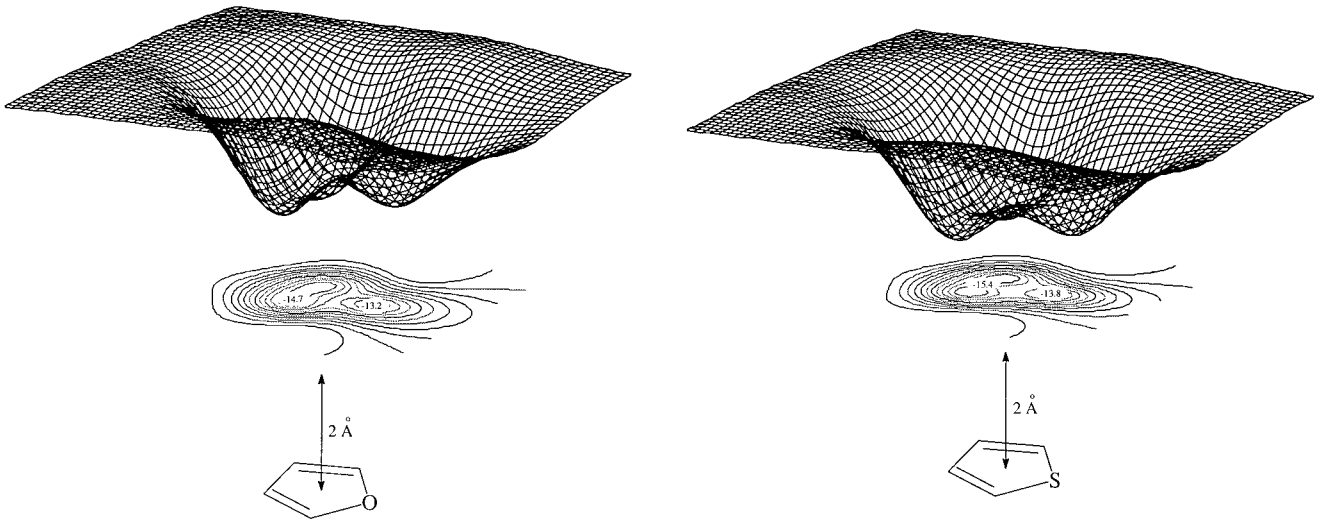

Figure 14. Out-of-plane electrostatic potential surfaces and maps (kcal/mol) 2 Å from (a, top) the furan (**13**, C_{2v}) ring plane and (b, bottom) the thiophene (**12**, C_{2v}) ring plane (RHF/6-31+G*//RB3LYP/6-31+G*).

filtered from lithium chloride precipitate. Distillation (80 mbar/104 °C) of the resulting solution afforded 9.53 g (0.054 mol, 90%) of **ClSiMe$_2$(2-C$_4$H$_3$S)**, which was subsequently dissolved in 50 mL of diethyl ether. This ether solution was slowly added to a mixture of 10 g of $NaHCO_3$ in 100 mL of H_2O at pH ∼7−5 (indicator).[31] Extraction with diethyl ether, drying over Na_2SO_4 and distillation yielded 6.16 g (0.039 mol) of **HOSiMe$_2$(2-C$_4$H$_3$S)** (65%): bp 55 °C/1 mbar; ^{1}H NMR ($CDCl_3$) δ 7.54 (d, C$_4$*H*$_3$S), 7.28 (d, C$_4$*H*$_3$S), 7.13 (t, C$_4$*H*$_3$S), 4.20 (s, *H*O−Si), 0.35 (s, Si−C*H*$_3$); ^{13}C{^{1}H} NMR ($CDCl_3$) δ 138.46, 134.59, 130.82, 128.01, 0.76; IR (neat, cm^{-1}) 3300 (O−H), 2970 (C−H Me).

Lithiation of **HOSiMe$_2$(2-C$_4$H$_3$S)** with n-BuLi (1.6 M) (1:1) in hexane solution (−20 °C, then 5 min at room temperature) afforded **Li−O−SiMe$_2$(2-C$_4$H$_3$S) (6)** (95%): ^{1}H NMR ($CDCl_3$) δ 7.52 (d, C$_4$*H*$_3$S), 7.20 (d, C$_4$*H*$_3$S), 7.13 (t, C$_4$*H*$_3$S), 0.08 (s, Si−C*H*$_3$); ^{13}C{^{1}H} NMR ($CDCl_3$) δ 143.24, 133.02, 129.83, 128.66, 2.81; MS (EI, 70 eV, 140 °C) *m*/*e* 984 ([M]$_6^+$), 969 ([M]$_6^+$ − Me), 641 ([M]$_4^+$ − Me), 313 ([M]$_2^+$ − Me), 171 ([M] − Li$^+$). Anal. Calcd for $C_6H_9OSLiSi$: C, 43.9; H, 5.5. Found: C, 43.5, H, 5.8. Single crystals of **6** were obtained from cooled hexane solutions.

(31) For the synthesis of silanoles from chlorosilanes see, for example: Pawlenko, S. *Methods of Organic Chemistry (Houben-Weyl)*, 4th ed.; Thieme: Stuttgart, Germany, 1980; Vol. 13,5, p 135.

X-ray crystal data for (**6**)$_6$: M_r = 164.22; monoclinic; space group $P2_1/n$; a = 12.698(5) Å, b = 18.192(6) Å, c = 13.469(5) Å; V = 2817(2) Å^3; D_{calcd} = 1.162 Mg m^{-3}; Z = 12; $F(000)$ = 1032; Mo Kα (λ = 0.710 73 Å); T = 200(2) K; crystal size 0.50 × 0.50 × 0.40 mm; 4° < 2θ < 52°; 6401 reflections collected; 5564 independent reflections, $I > 2\sigma(I)$; 2117 data; 273 refined parameters. Final R values: R1 = 0.0823 ($I > 2\sigma(I)$) and wR2 = 0.2654 (all data); GOF = 0.831; largest peak 0.508 e Å^{-3}; largest and hole −0.508 e Å^{-3}.

In the X-ray crystal structure of compound (**6**)$_6$, the thienyl ring atoms C_3, C_4, and S exhibit large anisotropic displacement parameters (U). Assumed disordered positions (S at C_3 or C_4) could not be verified by refinement. Disordered S at C_3 or C_4 is also excluded by ortho-substitution relative to S at C_1. The ring atom C_2 has normal displacements, excluding disordered S at this C_2 position. The ring atoms with large U values are displaced mainly *in the plane* of the thienyl rings. These in-plane displacements affect the bond distances within the thienyl rings but do not influence the torsions of the thienyl moieties.

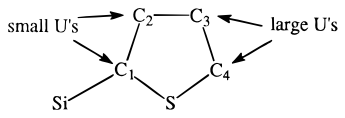

Li−O−CH(*i*-Pr)(2-C_4H_3S) (9). A solution of 5.4 g (0.06 mol) of 2-lithiothiophene in THF/hexane was prepared from 37.5 mL (0.06 mol) of BuLi (1.6 M in hexane) and 6.05 g (0.072 mol) of thiophene in 50 mL of THF.[30] To this solution was added 4.3 g (0.06 mol) of isobutyraldehyde (HCO-*i*-Pr) in 100 mL of diethyl ether dropwise at 0 °C. After the resulting mixture was stirred at room temperature for 1 h, hydrolysis with H_2O/NH_4Cl, extraction with diethyl ether, drying over Na_2SO_4, and distillation afforded 8.6 g (0.055 mol) of **HOCH(*i*-Pr)(2-C_4H_3S)** (91% yield): bp 58 °C/1 mbar; ^{1}H NMR ($CDCl_3$) δ 7.16 (d, C_4H_3S), 6.89 (t, C_4H_3S), 6.86 (d, C_4H_3S), 2.92 (s, *H*O), 1.92 (sept, C*H*), 0.97, 0.81 (each d, CH_3); ^{13}C{^{1}H} NMR ($CDCl_3$) δ 147.66, 126.28, 124.16, 124.13, 75.62, 35.72, 18.82, 18.36; ^{13}C CP-MAS δ 155.61, 124.94, 124.95, 78.36, 40.45, 22.16, 20.51; IR (neat, cm^{-1}) 3440 (O−H), 3100, 3120 (C−H thiophene), 2980 (C−H aliphatic).

Lithiation of **HOCH(*i*-Pr)(2-C_4H_3S)** with *n*-BuLi (1.6 M) (1:1) in hexane solution (−20 °C, then 5 min at room temperature) afforded **Li−O−CH(*i*-Pr)(2-C_4H_3S) (9)** (92%): ^{1}H NMR ($CDCl_3$) δ 7.13 (d, C_4H_3S), 6.92 (t, C_4H_3S), 6.70 (d, C_4H_3S), 1.37 (m, C*H*), 0.81, 0.58 (each d, CH_3); ^{13}C{^{1}H} NMR ($CDCl_3$) δ 154.65, 126.85, 122.74, 122.55, 76.69, 38.64, 20.12, 18.73; MS (EI, 70 eV, 110 °C) *m*/*e* 817 ([M]$_5$ − Li$^+$), 493 ([M]$_3$ − Li$^+$), 169 ([M] − Li$^+$); Anal. Calcd for $C_8H_{11}OSLi_1$: C, 59.2; H, 6.8. Found: C, 59.0; H, 6.9. Single crystals of **9** were obtained from cooled hexane solutions.

X-ray crystal data for (**9**)$_6$: M_r = 162.17; hexagonal; space group $R\bar{3}$; a = 19.999(5) Å, b = 20.00(5) Å, c = 11.842(10) Å; V = 4102(11) Å^3; D_{calcd} = 1.182 Mg m^{-3}; Z = 18; F(000) = 1548; Mo Kα (λ = 0.710 73 Å); T = 200(2) K; crystal size 0.50 × 0.40 × 0.30 mm; 4° < 2θ < 54°; 2748 reflections collected; 2045 independent reflections, $I > 2\sigma(I)$; 734 data; 108 refined parameters. Final R values: R1 = 0.0708 ($I > 2\sigma(I)$) and wR2 = 0.2754 (all data); GOF = 0.925; largest peak 0.409 e Å^{-3}, largest hole −0.397 e Å^{-3}. Carbon atoms of the *i*-Pr groups in the X-ray structure of (**9**)$_6$ are disordered.

Theoretical Methods

The theoretical structures were optimized with Becke's three-parameter hybrid functional[32] incorporating the Lee−Yang−Parr correlation functional[33] (Becke3LYP) using the gradient techniques implemented in GAUSSIAN 94.[34] The 6-31G*, 6-31+G*, 6-311+G*, and 6-311+G** basis sets were employed. The character of the stationary points and the zero-point energy correction were obtained from analytical frequency calculations. The PM3 method[16a] implemented in VAMP 5.0[35] with the lithium parameters of Anders et al.[16b] was used. The electrostatic potentials were evaluated with RHF/6-31+G* wave functions on optimized RB3LYP geometries.

Acknowledgment. This work was supported by the Fonds der Chemischen Industrie (also through a scholarship to B.G.), the Stiftung Volkswagenwerk, Convex Computer Corp., and the Deutsche Forschungsgemeinschaft.

Supporting Information Available: Tables giving crystal data and structure refinement details, atomic coordinates, bond distances and angles, and thermal parameters for (**6**)$_6$ and (**9**)$_6$ (17 pages). Ordering information is given on any current masthead page.

OM9703604

(32) Becke, A. D. *J. Chem. Phys.* **1993**, *98*, 5648.
(33) Lee, C.; Yang, W.; Parr, R. G. *Phys. Rev. B* **1988**, *37*, 785.
(34) Frisch, M. J.; Trucks, G. W.; Schlegel, H. B.; Gill, P. M. W.; Johnson, B. G.; Robb, M. A.; Cheeseman, J. R.; Keith, T.; Petersson, G. A.; Montgomery, J. A.; Raghavachari, K.; Al-Laham, M. A.; Zakrzewski, V. G.; Ortiz, J. V.; Foresman, J. B.; Cioslowski, J.; Stefanov, B. B.; Nanayakkara, A.; Challacombe, M.; Peng, C. Y.; Ayala, P. Y.; Chen, W.; Wong, M. W.; Andres, J. L.; Replogle, E. S.; Gomperts, R.; Martin, R. L.; Fox, D. J.; Binkley, J. S.; Defrees, D. J.; Baker, J.; Stewart, J. P.; Head-Gordon, M.; Gonzalez, C.; Pople, J. A. Gaussian 94, Revision C.3, Gaussian, Inc., Pittsburgh PA, 1995.
(35) Rauhut, G.; Alex, A.; Chandrasekhar, J.; Steinke, T.; Clark, T. VAMP Version 5.00; Erlangen, Germany, 1993.
(36) Hellwege, K. H., Ed. *Landolt-Börnstein Numerical Data and Functional Relationships in Science and Technology*; Springer-Verlag: Heidelberg, Germany, 1974; Group II, Vol. 6 (Molecular Constants).
(37) (a) Reed, A. E.; Curtiss, L. A.; Weinhold, F. *Chem. Rev.* **1988**, *88*, 899. (b) Reed, A. E.; Schleyer, P. v. R. *J. Am. Chem. Soc.* **1990**, *112*, 1434.
(38) Mulliken, R. S. *J. Chem. Phys.* **1955**, *23*, 1833.
(39) (a) Besler, B. H.; Merz, K. M., Jr.; Kollman, P. A. *J. Comput. Chem.* **1990**, *11*, 431. (b) Singh, U. C.; Kollman, P. A. *J. Comput. Chem.* **1984**, *5*, 129.
(40) Breneman, C. M.; Wiberg, K. B. *J. Comput. Chem.* **1990**, *11*, 361.
(41) Nelson, R. D.; Lide, D. R.; Maryott, A. A. *Selected Values of Electric Dipole Moments in the Gas Phase*, Natl. Stand. Ref. Data Ser.-Natl. Bur. Std. 10; National Bureau of Standards: Washington, DC, 1967.
(42) Hehre, W. J.; Radom, L.; Schleyer, P. v. R.; Pople, J. A. *Ab Initio Molecular Theory*; Wiley: New York, 1985.